MYCOLOGIA

Mycologia

ISSN: (Print) (Online) Journal homepage: https://www.tandfonline.com/loi/umyc20

Fusarium abutilonis and *F. guadeloupense*, two novel species in the *Fusarium buharicum* clade supported by multilocus molecular phylogenetic analyses

Kerry O'Donnell, Tom Gräfenhan, Imane Laraba, Mark Busman, Robert H. Proctor, Hye-Seon Kim, Nathan P. Wiederhold, David M. Geiser & Keith A. Seifert

To cite this article: Kerry O'Donnell, Tom Gräfenhan, Imane Laraba, Mark Busman, Robert H. Proctor, Hye-Seon Kim, Nathan P. Wiederhold, David M. Geiser & Keith A. Seifert (2022) *Fusarium abutilonis* and *F. guadeloupense*, two novel species in the *Fusarium buharicum* clade supported by multilocus molecular phylogenetic analyses, Mycologia, 114:4, 682-696, DOI: 10.1080/00275514.2022.2071563

To link to this article: https://doi.org/10.1080/00275514.2022.2071563

MYCOLOGIA
2022, VOL. 114, NO. 4, 682–696
https://doi.org/10.1080/00275514.2022.2071563

Taylor & Francis
Taylor & Francis Group

Fusarium abutilonis and *F. guadeloupense*, two novel species in the *Fusarium buharicum* clade supported by multilocus molecular phylogenetic analyses

Kerry O'Donnell[a], Tom Gräfenhan[b,c], Imane Laraba[a], Mark Busman[a], Robert H. Proctor[a], Hye-Seon Kim[a], Nathan P. Wiederhold[d], David M. Geiser[e], and Keith A. Seifert[b,f]

[a]Mycotoxin Prevention and Applied Microbiology Research Unit, National Center for Agricultural Utilization Research, Agricultural Research Service, United States Department of Agriculture, 1815 N. University St. 61604, Peoria, Illinois 61604-3999; [b]Biodiversity (Mycology & Botany), Ottawa Research and Development Centre, Agriculture and Agri-Food Canada, ON K1A 0C6, Ottawa, Ontario, Canada; [c]Core Unit Systems Medicine, Medical Faculty, Josef-Schneider-Str. 2, Gebäude 2, University of Würzburg, Würzburg 97080, Germany; [d]Department of Pathology and Laboratory Medicine, 7703 Floyd Curl Drive, University of Texas Health Science Center at San Antonio, San Antonio, Texas 78229, USA; [e]Department of Plant Pathology and Environmental Microbiology, Pennsylvania State University, 121 Buckhout Lab, University Park, Pennsylvania 16802, USA; [f]Department of Biology, Carleton University, ON K1S 5B6, Ottawa, Ontario, Canada

ABSTRACT

This study was conducted to elucidate evolutionary relationships and species diversity within the *Fusarium buharicum* species complex (FBSC). We also evaluate the potential of these species to produce mycotoxins and other bioactive secondary metabolites. Maximum likelihood and maximum parsimony analyses of sequences from portions of four marker loci (ITS rDNA, *TEF1*, *RPB1*, and *RPB2*) and the combined 4495 bp data set support recognition of seven genealogically exclusive species within the FBSC. Two of the three newly discovered species are formally described as *F. abutilonis* and *F. guadeloupense* based on concordance of gene genealogies and morphological data. *Fusarium abutilonis* induces leaf, stem, and root lesions on several weedy Malvaceae (*Abution theophrasti, Anoda cristata, Sida spinosa*) and a fabaceous host (*Senna obtusifolia*) in North America and also was recovered from soil in New Caledonia. *Fusarium abutilonis*, together with its unnamed sister, *Fusarium* sp. ex common marsh mallow (*Hibiscus moscheutos*) from Washington state, and *F. buharicum* pathogenic to cotton and kenaf in Russia and Iran, respectively, were strongly supported as a clade of malvaceous pathogens. The four other species of the FBSC are not known to be phytopathogenic; however, *F. guadeloupense* was isolated from human blood in Texas and soil in Guadeloupe. The former isolate is unique because it represents the only known case of a fusarial infection disseminated hematogenously by a species lacking microconidia and the only documented fusariosis caused by a member of the FBSC. Whole genome sequence data and extracts of cracked maize kernel cultures were analyzed to assess the potential of FBSC isolates to produce mycotoxins, pigments, and phytohormones.

ARTICLE HISTORY
Received 6 January 2022
Accepted 26 April 2022

KEYWORDS
Chlamydospores; equisetin; genealogical concordance phylogenetic species recognition (GCPSR); morphology; *RPB1*; *RPB2*; sporodochial conidia; *TEF1*; whole genome sequence; 2 new taxa

INTRODUCTION

Fusarium (Hypocreales, Nectriaceae) is widely recognized as the most important group of mycotoxigenic plant pathogens, and also as an emergent opportunistic pathogen of immunocompromised and artificially immunosuppressed patients (Summerell 2019). *Fusarium* diseases and their toxins are responsible for multibillion US dollar losses to the world's agricultural economy, caused by yield reduction and toxin contamination of commodities that are unsuitable for food and feed. Ongoing multilocus molecular phylogenetic analyses of fusaria housed in the Agricultural Research Service (ARS) Culture Collection (NRRL; Peoria, Illinois), the Fusarium Research Center (FRC; Pennsylvania State University, University Park, Pennsylvania), and the Westerdijk Fungal Biodiversity Institute (CBS-KNAW; Utrecht, the Netherlands) indicate that this agronomically important genus comprises over 450 phylospecies distributed among 23 monophyletic species complexes (Geiser et al. 2021, 2013; O'Donnell et al. 2013). The marriage of polymerase chain reaction (PCR) and automatic DNA sequencing technologies, and broad acceptance of phylogenetic species recognition based on genealogical concordance (GCPSR; sensu Taylor et al. 2000), has been largely responsible for the discovery and formal recognition of ~250 phylospecies over the past two decades (Aoki et al. 2014; Summerell 2019). Given the omnipresent threat that these pathogens and their structurally diverse mycotoxins (i.e., trichothecenes, zearalenone, fumonisins, and enniatins) pose to global agricultural biosecurity, food safety, and human health, detailed molecular systematic studies published over the past quarter century

CONTACT Kerry O'Donnell kerry.odonnell@usda.gov
Supplemental data for this article can be accessed on the publisher's Web site.

Published online 09 Jun 2022

have focused on the largest and most important mycotoxin-producing and phytopathogenic lineages, including the *F. sambucinum* (Laraba et al. 2021), *F. fujikuroi* (Nirenberg and O'Donnell 1998; O'Donnell et al. 1998a; Yilmaz et al. 2021), *F. solani* (O'Donnell 2000; Sandoval-Denis and Crous 2018), *F. oxysporum* (O'Donnell et al. 2009), and *F. tricinctum* (Laraba et al. 2022) species complexes as defined in O'Donnell et al. (2013) and Geiser et al. (2021).

These GCPSR-based multilocus molecular phylogenetic studies clearly establish that morphological species recognition (MSR) greatly underestimates species diversity within *Fusarium* (Booth 1971; Gerlach and Nirenberg 1982; Nelson et al. 1983; Wollenweber and Reinking 1935). They also revealed that the morphology-based subgeneric sectional classification (Wollenweber and Reinking 1935) adopted in most taxonomic treatments of the genus is nonmonophyletic (see O'Donnell et al. 2013). Section Discolor, for example, was erected to include fusaria with thick-walled sporodochial conidia, chlamydospore production, and the absence of microconidia; however, it is a paraphyletic assemblage of phylogenetically diverse species from several species complexes (i.e., *Buharicum, Fujikuroi, Heterosporum, Sambucinum*, and *Tricinctum*).

Because morphological species recognition within *Fusarium* has significant limitations, preliminary identifications of a broad sampling of fusaria housed in NRRL, FRC, and CBS-KNAW were obtained by conducting BLASTn searches of FUSARIUM-ID (http://isolate.fusariumdb.org/blast.php; Geiser et al. 2004), *Fusarium MLST* (http://www.westerdijkinstitute.nl/fusarium/; O'Donnell et al. 2010), and National Center for Biotechnology Information (NCBI) GenBank (http://www.ncbi.nlm.nih.gov/; O'Donnell et al. 2015), using partial translation elongation factor 1-α (*TEF1*) sequences as the queries. Results of these searches indicate that several isolates in these collections appear to represent putatively undescribed species within the *F. buharicum* species complex (FBSC).

The FBSC currently comprises three formally described species: *Fusarium buharicum* (Gerlach and Scharif 1970; Jaczewski 1929), *F. convolutans* (Sandoval-Denis et al. 2018), and *F. sublunatum* (Reinking 1934); however, no detailed molecular phylogenetic analyses of the FBSC have been conducted. Therefore, the present study was initiated to (i) investigate evolutionary relationships among and species diversity within this complex, (ii) formally describe two phylospecies that fulfill the exclusivity criterion of reciprocal monophyly under GCPSR, (iii) assess the potential of six species within the FBSC to produce mycotoxins and other biologically active secondary metabolites by conducting in silico analyses of whole genome sequence data, and (iv) determine whether members of this complex produce mycotoxins, based on a cracked maize kernel culture assay using high-performance liquid chromatography–mass spectrometry (HPLC-MS) analyses.

MATERIALS AND METHODS

Fungal isolates.— Histories of the two novel species formally described in the present study, *Fusarium abutilonis* and *F. guadeloupense*, together with those of five other members of the *F. buharicum* species complex (FBSC) and two outgroups from the *F. torreyae* species complex (*F. torreyae* and *F. xanthoxyli*; Zhou et al. 2018), are included in TABLE 1. The eight strains of *F. abutilonis* were isolated from three weedy members of the Malvaceae (*Abutilon theophrasti*, velvetleaf; *Anoda cristata*, crested or spurred anoda; and *Sida spinosa*, prickly sida), a fabaceous weed (*Senna obtusifolia*, sicklepod), and soil in New Caledonia (TABLE 1). Pure cultures of *F. abutilonis* from several weeds collected in Mississippi were previously reported as *F. lateritium* (Walker 1981), and *F. guadeloupense* NRRL 36125 from Guadeloupe was deposited by H. Anders as *F. sublunatum* in the Institute for Epidemiology and Pathogen Diagnostics Culture Collection Berlin, Germany (BBA 70872), and Westerdijk Fungal Biodiversity Institute (CBS 102302). The second strain of *F. guadeloupense* NRRL 66743 was recovered from human blood in Texas and deposited in the Fungus Testing Laboratory, University of Texas Health Science Center at San Antonio, as *Fusarium* sp. UTHSC DI14-24.

Colony and conidial features were characterized by culturing isolates on synthetic low nutrient agar (SNA; Nirenberg 1976) with filter paper (Whatman, grade 4; Sigma-Aldrich, St. Louis, Missouri) and potato dextrose agar (PDA; Difco, Detroit, Michigan). Isolates were grown in the dark at room temperature (20–22 C) or under an alternating 12 h dark/12 h black (near-ultraviolet [near-UV]) light cycle at 25 C. Photo documentation and measurements of macroconidia and chlamydospores were taken from SNA cultures mounted in water (Gräfenhan et al. 2016). Isolates were cultured on PDA in 9-cm Petri dishes in the dark at room temperature to study colony morphology, and Kornerup and Wanscher (1978) was used as the source of alphanumeric codes to describe color. Mycelial growth rates were determined by culturing strains for 7 d in the dark on PDA and SNA at 25 C. Strains included in this study were accessioned in

Table 1. Histories of strains included in this study and mycotoxin production.

Fusarium species[a]	NRRL and KOD nos.[b]	Equivalent no.[c]	Host/substrate	Geographic origin	Equisetin (ng/mL)[d]
F. abutilonis	NRRL 13279	FRC L-0105	*Anoda cristata*	Mississippi, USA	None detected
F. abutilonis	NRRL 54621	FRC L-0115	*Anoda cristata*	Mississippi, USA	None detected
F. abutilonis	NRRL 54622	FRC L-0118	*Anoda cristata*	Mississippi, USA	None detected
F. abutilonis	NRRL 54627	FRC L-0215	*Sida spinosa*	Mississippi, USA	None detected
F. abutilonis	NRRL 54654	FRC L-0117	*Abutilon theophrasti*	Mississippi, USA	None detected
F. abutilonis	NRRL 54680	FRC L-0271	*Senna obtusifolia*	Mississippi, USA	None detected
F. abutilonis	**NRRL 66737 [T]**	DAOMC 213370	*Abutilon theophrasti*	Ontario, Canada	None detected
F. abutilonis	NRRL 66738 = KOD 928	BBA 69700	*Abutilon theophrasti*	Ontario, Canada	None detected
F. abutilonis	BBA 65832	None	soil, clay; soybean rhizosphere	New Caledonia	—
F. abutilonis	BBA 65925	None	soil, clay	New Caledonia	—
F. buharicum	**NRRL 13371**	FRC R-4955 = CBS 796.70	*Hibiscus cannabinus*	Iran	None detected
F. buharicum	NRRL 25488	CBS 178.35	*Gossypium* sp.	Russia	—
F. convolutans	KOD 1954	CBS 144207	*Kyphocarpa angustifolia* rhizophere	South Africa	—
F. convolutans	KOD 1955	CBS 144208	*Kyphocarpa angustifolia* rhizophere	South Africa	None detected
F. guadeloupense	**NRRL 36125 [T]**	CBS 102302 = BBA 70872	Soil	Guadeloupe	None detected
F. guadeloupense	NRRL 66743 = KOD 749	UTHSC DI14-24	Human blood	Texas, USA	None detected
F. sublunatum	**NRRL 13384 = KOD 675 [T]**	CBS 189.34	Soil	Costa Rica	9.88
F. sublunatum	NRRL 20897	CBS 190.34	Soil	Costa Rica	13.02
Fusarium sp.	**NRRL 66739 = KOD 1155**	FRC L-0453	unknown	China	—
Fusarium sp.	NRRL 66179 = KOD 935	WRPIS 2012–95	*Hibiscus moscheutos*	Washington, USA	None detected
Fusarium sp.	**NRRL 66182 = KOD 938**	WRPIS 2013–63	*Hibiscus moscheutos*	Washington, USA	None detected
F. torreyae	NRRL 54151 [T]	MAFF 243468	*Torreya taxifolia*	Florida, USA	—
F. zanthoxyli	**NRRL 66285 [T]**	CBS 140838	*Zanthoxylum bungeanum*	China	—

[a]All of the species are members of the *F. buharicum* species complex except for *F. torreyae* and *F. zanthoxyli*, which are outgroups.
[b]NRRL = ARS Culture Collection, NCAUR, Peoria, Illinois; KOD = strain accession stored in Kerry O'Donnell laboratory at NCAUR. Whole genomes were obtained for those strains listed in bold. [T] = ex-type strain.
[c]BBA = Biologische Bundesanstalt für Land- und Forstwirtschaft, Institut für Mikrobiologie, Berlin, Germany; CBS = Westerdijk Fungal Biodiverity Institute, Utrecht, The Netherlands; DAOMC = Canadian Collection of Fungal Cultures, Ottawa, Canada; FRC = Fusarium Research Center, The Pennsylvania State University, University Park, Pennsylvania; KAS = Keith A. Seifert strain accession numbers, Ag-Canada, Ottawa, Canada; MAFF = Ministry of Agriculture and Forestry, NIAS, Tsukuba, Japan; UTHSC = University of Texas Health Sciences Center, San Antonio, Texas; WRPIS = Western Regional Plant Introduction Station, Pullman, Washington.
[d]Equisetin (ng/mL) produced in vitro on solid cracked maize kernal culture. —, not tested.

the ARS Culture Collection (NRRL; TABLE 1) where they are available for distribution upon request (https://nrrl.ncaur.usda.gov/).

Genomic DNA extraction, PCR amplification, and sequencing.—Total genomic DNA was extracted from mycelium cultured in yeast-malt broth (3 g yeast extract, 3 g malt extract, 5 g peptone, 20 g dextrose per L) for 3–5 d, freeze-dried, and then extracted using a CTAB (cetyl trimethylammonium bromide) protocol (Gardes and Bruns 1993). Portions of the following four marker loci were PCR amplified and Sanger sequenced: nuclear ribosomal internal transcribed spacer region (ITS rDNA), translation elongation factor 1-α (*TEF1*), and DNA-directed RNA polymerase I largest (*RPB1*) and second largest (*RPB2*) subunits. Amplicons were obtained using the following primer pairs: ITS5 (GGAAGTAAAAGTCGTAACAAGG) × ITS4 (TCCTCCGCTTATTGATATGC) (White et al. 1990) for ITS rDNA; EF-1 (5′-ATGGGTAAGGARGACAAGAC-3′) × EF-2 (5′-GGARGTACCAGTSATCATG-3′) for *TEF1* (O'Donnell et al. 1998b); Fa (5'-CAYAARGARTCYATGATGGGWC-3′) × G2R (5'-GTCATYTGDGTDGCDGGYTCDCC-3') for *RPB1* (O'Donnell et al. 2010); and 5f2 (5′-GGGGWGAYCAGAAGAAGGC-3′) × 7cr (CCCATRGCTTGYTTRCCCAT-3′) and 7cf (5'- ATGGGYAARCAAGCYATGGG-3′) × 11ar (5-′GCRTGGATCTTRTCRTCSACC-3′) for *RPB2* (Liu et al. 1999; Reeb et al. 2004). Amplicons were obtained following published protocols (Laraba et al. 2018; O'Donnell et al. 2010; White et al. 1990) in a ProFlex thermocycler (ABI, Emeryville, California) and purified using ExoSAP-IT (ABI) after aliquots of the PCR reactions were checked using electrophoresis in 1.5% agarose gels. After amplicons were sequenced using ABI BigDye 3.1 Terminator reaction mix, they were purified using ABI BigDye XTerminator and then run on an ABI 3730 48-capillary DNA analyzer. ABI sequence chromatograms were edited using Sequencher 5.2.4 (Gene Codes, Ann Arbor, Michigan) and exported as FASTA files that were aligned using MUSCLE (Edgar 2004) in SeaView 4.7 (Gouy et al. 2009). Sequences were used to conduct BLASTn queries of NCBI GenBank (https://www.ncbi.nlm.nih.gov/genbank/), FUSARIUM-ID (http://isolate.fusariumdb.org/blast.php; Geiser et al. 2004), and *Fusarium MLST* (https://fusarium.mycobank.org/) to obtain preliminary identifications (O'Donnell et al. 2015).

Phylogenetic analyses.—The multilocus sequence data collected for *F. abutilonis* and *F. guadeloupense* were aligned with sequences previously published and deposited in NCBI GenBank for five FBSC species (Lupien et al. 2017; O'Donnell et al. 2013; Sandoval-Denis et al. 2018)

and two outgroups (TABLE 1) (Aoki et al. 2013; Zhou et al. 2018). The latter were selected for rooting the trees based on more inclusive analyses (Geiser et al. 2021; SUPPLEMENTARY FIG. 1, SUPPLEMENTARY FILE 1). Aligned sequences from the four individual partitions were analyzed with maximum likelihood bootstrapping (ML-BS) using IQ-TREE 1.6.12 (Nguyen et al. 2015; http://www.iqtree.org/) to determine the best-fit model of molecular evolution. The latter were based on the Bayesian information criterion (BIC) scores (Chernomor et al. 2016) using ModelFinder (Kalyaanamoorthy et al. 2017). Once the optimal models were determined, a partitioned ML-BS analysis was conducted with IQ-TREE in which 5000 pseudoreplicates were run to assess statistical support for evolutionary relationships among the lineages and species monophyly (TABLE 2). Clade support was also assessed using maximum parsimony bootstrap (MP-BS) analyses of the four individual partitions and combined data set with PAUP* 4.0a.168 (http://phylosolutions.com/paup-test/). PAUP* was also used to assess the species status of *Fusarium* sp. NRRL 66738 from China by determining percent nucleotide divergence between it and its putative sister, *F. sublunatum* NRRL 13384, based on analyses of (i) the four individual partitions and combined data set (TABLE 3), and (ii) alignments of 19 individual genes mined from the genomes of *Fusarium* sp. NRRL 66738 and *F. sublunatum* NRRL 13384, and the combined 20-gene 60.4 kb data set (TABLE 4; Geiser et al. 2021). DNA sequences generated in the present study were deposited in NCBI (accession nos. OM117592–OM117610 and OM160817–OM160879) and FUSARIUM-ID 3.0 (Torres-Cruz et al. 2022).

Whole genome sequencing.—Genomic DNA for the strains was prepared using the ZR Fungal/Bacterial DNA MiniPrep Kit (Zymo Research, Irvine, California). The DNA was processed into libraries with an average insert size of 300 bases using a Nextera XT Kit (Illumina, San Diego, California). The libraries were sequenced using a MiSeq instrument as specified by the manufacturer (Illumina). Sequence reads were processed and assembled with CLC Genomics Workbench (CLC) 12.0 (CLC bio-Qiagen, Aarhus, Denmark). Prior to de novo assembly, reads were screened against genome sequences of 84 bacterial species and sequences of Nextera adapters to remove contaminating DNA. The reads were also trimmed to remove low-quality bases at either end. De novo assembly of the reads was accomplished using the following CLC settings: word size of 20; bubble size of 50; minimum contig length of 500; autodetect paired distances; and perform scaffolding. The ab initio gene prediction method implemented in AUGUSTUS, using *F. graminearum* data as a reference, was used to predict proteins encoded by each genome sequence (Stanke and Morgenstern 2005). antiSMASH (3.0 and 4.0) was then used to identify secondary metabolite biosynthetic gene clusters in the genome sequences (Blin et al. 2017). The presence or absence of some gene clusters was confirmed by BLASTn analysis as implemented in CLC using previously described biosynthetic genes as queries (Laraba et al. 2018; Niehaus et al. 2016). Genome sequence data were generated for seven members of the FBSC and deposited in NCBI GenBank: *F. guadeloupense* NRRL 36125 (JAJJWL000000000), *F. guadeloupense* NRRL 66743 (JAJJWM000000000),

Table 2. *Buharicum* clade loci sequenced and monophyly support.

		ML-BS/MP-BS support (%)[b]					
Locus	PICs/bp/% PIC[a]	*F. abutilonis*	*F. buharicum*	*F. convolutans*	*F. guadeloupense*	*F. sublunatum*	*Fusarium* sp. NRRL 66179
ITS rDNA[b]	27/491/5.5	</<	</<	—/—	100/100	87/87	83/80
TEF1	164/685/23.9	78/89	100/100	100/100	100/100	94/98	100/100
RPB1	311/1575/19.7	93/100	100/100	100/100	100/100	91/98	100/100
RPB2	345/1744/19.8	99/100	100/100	100/100	100/100	81/99	100/100
Combined	847/4495/18.8	97/100	100/100	100/100	100/100	98/100	100/100

Note. <, less than 70% bootstrap support; —, not evaluated due to missing data.
[a]No. of parsimony-informative characters (PICs)/no. base pairs(bp)/% PIC.
[b]Maximum likelihood bootstrap support (%)/maximum parsimony bootstrap support (%) based on 5000 pseudoreplicates of the data.

Table 3. Divergence between *Fusarium sublunatum* NRRL 13384 and *Fusarium* sp. NRRL 66739.

4-gene (FIG. 1)	Locus identifier	bp alignment	Steps	% divergence
ITS rDNA	Nuclear ribosomal ITS region	491	9	1.8
TEF1	Translation elongation factor 1-alpha	685	13	1.9
RPB1	RNA polymerase largest subunit	1575	12	0.8
RPB2	RNA polymerase 2nd largest subunit	1744	24	1.4
Combined	4 loci combined	4495	58	1.3

Table 4. Divergence between *Fusarium sublunatum* NRRL 13384 and *Fusarium* sp. NRRL 66739 based on maximum parsimony analyses of 20 full-length genes.

Locus	Protein encoded	bp alignment	Steps	% divergence
acl1	ATP citrate lyase large subunit	1883	21	1.1
act1	Actin	1494	47	3.1
cal1	Calmodulin	974	23	2.4
cpr1	Cytochrome P450 reductase	2205	40	1.8
dpa1	DNA polymerase alpha subunit	4593	84	1.8
dpe1	DNA polymerase epsilon subunit	6883	132	1.9
fas1	Fatty acid synthase alpha subunit	5696	75	1.3
fas2	Fatty acid synthase beta subunit	6367	55	0.9
ku70	ATP-dependent DNA helicase II	2043	37	1.8
lcb2	Sphinganine palmitoyl transferase subunit	1992	31	1.6
mcm7	DNA replication licensing factor	2674	34	1.3
pgk1	Phosphoglycerate kinase	1580	45	2.8
pho	Phosphate permase	1905	100	5.2
rpb1	RNA polymerase largest subunit	5379	57	1.1
rpb2	RNA polymerase 2nd largest subunit	3916	59	1.5
tef1	Translation elongation factor 1-alpha	1791	17	0.9
top1	Topoisomerase	3131	63	2
tsr1	Ribosomal biogenesis protein	2513	81	3.2
tub1	Tubulin alpha subunit	1731	15	0.7
tub2	Tubulin beta subunit	1687	41	2.4
Combined	20 genes combined	60 437	1057	1.75

F. abutilonis NRRL 66737 (JAJJWN000000000), *Fusarium* sp. NRRL 66739 (JAJJWO000000000), *F. buharicum* NRRL 13371 (JAATHB000000000), *F. sublunatum* NRRL 13384 (JABFFF000000000), and *Fusarium* sp. NRRL 66182 (JABFAK000000000).

Determination of secondary metabolite biosynthetic potential.— Previously described methods were used to screen the *F. buharicum* clade strains for production of mycotoxins and other secondary metabolites (Aoki et al. 2015). After 14 d incubation in the dark on cracked maize kernels, 10 g from each culture was extracted with 20 mL 86:14 (*v*/*v*) acetonitrile:water for 30 min with shaking. Once the extracts were clarified by filtration, they were analyzed by high-performance liquid chromatography–mass spectrometry (HPLC-MS) using a Dionex Ultimate U3000 liquid chromatography system coupled to a Q Exactive high-resolution mass spectrometer equipped with an electrospray ionization (ESI) source (Thermo Fisher Scientific, Waltham, Massachusetts). A Phenomenex Kinetex 2 mm × 50 mm XB-C18 100A column (2.6 µm particle size, 100 Å pore size; Phenomenex Inc., Torrance, California) was used to separate the metabolites. After injecting 10 µL of each extract, metabolites were eluted in a binary gradient flow of mobile phase A (water: acetic acid 99.7:0.3 *v*/*v*) and mobile phase B (methanol: acetic acid 99.7:0.3 *v*/*v*). The mobile phase B gradient of 20–95% was delivered over 5 min at a flow rate of 0.6 mL/min. The mass spectrometer to which the HPLC was connected was operated in positive mode utilizing the following parameters: 320 C capillary temperature, 310 C heater temperature, and spray voltage of 4.00 kV for positive ESI. In addition, the mass spectrometer was operated in full MS mode (*m*/*z* range 150–2000 and 70 000 resolution), followed by screening metabolite production as previously described (Busman 2017; Busman et al. 2012). Identification and quantification of equisetin production was performed by HPLC-MS comparison of ion mass and elution time to a purified standard (Cayman Chemical Company, Ann Arbor, Michigan). Further confirmation of equisetin identity was made by HPLC-MS/MS comparison of ion fragmentation with the purified standard. The limit of quantification for equisetin was 1 ng/µL. Instrument operation and data processing were done using Xcalibur data acquisition and interpretation software (Thermo Fisher Scientific).

RESULTS

Molecular phylogenetics.— A 4-gene data set comprising the entire ITS rDNA region (491 bp alignment, 27 parsimony-informative characters [PICs]) and portions of *TEF1* (685 bp alignment, 164 PICs), *RPB1* (1575 bp alignment, 311 PICs), and *RPB2* (1744 bp alignment, 345 PICs), totaling 4495 bp of aligned DNA sequence data, was constructed to assess species limits and evolutionary relationships within the FBSC (TABLE 1; Geiser et al. 2021). The 19 FBSC strains included in this study were chosen to represent their global genetic diversity based on preliminary molecular phylogenetic analyses of *TEF1* and/or *RPB2* and BLASTn queries of NCBI GenBank and *Fusarium MLST*. Maximum likelihood (ML) and maximum parsimony (MP) bootstrapping (BS) of the *TEF1* (SUPPLEMENTARY FIG. 2), *RPB1* (SUPPLEMENTARY FIG. 3), and *RPB2* (SUPPLEMENTARY FIG. 4) partitions

conducted with IQ-TREE (Nguyen et al. 2015) and PAUP* supported monophyly of the six species represented by two or more strains (TABLE 2). Although only three species were supported as genealogically exclusive in analyses of the ITS rDNA partition, monophyly of the six species represented by two or more strains received moderate to strong ML and MP bootstrap support from the three other loci (ML-BS/MP-BS = 78–100%/80–100%; TABLE 2) and none of the inferred gene genealogies contradicted species monophyly. BLASTn searches of NCBI, using ITS rDNA sequences as the queries, suggest that accession FJ892747 deposited as *Fusarium* sp. from tomato in Xuzhou, China, might be *F. abutilonis* based on 99.8% identity with the ITS rDNA sequence of *F. abutilonis* NRRL 54654. These queries also suggest that sequences deposited as *F. buharicum* from soil in India (MN796096) and wetland sediments in China (JX076965) and Hypocreales from a marine habitat in Hawaii (EF060423) may represent novel species diversity within the FBSC. When a partial *TEF1* sequence of a strain from China without a detailed history (NRRL 66739 = FRC L-0453) was used to query GenBank, it showed 100% identity to GenBank accession EU668363 *Fusarium* sp. FTP001, which was isolated from invasive alligator weed (*Alternanthera philoxeroides*) in China, suggesting that these strains might be conspecific. Similarly, a partial *TEF1* sequence of the ex-type strain of *F. convolutans* CBS 144207 (GenBank accession LT996094) from soil in South Africa showed 99.7% identity to strain *Fusarium* sp. PD2 from China (GenBank accession MN848239). The fact that the two mismatching nucleotide positions were near either end of the alignment, and potentially represent sequencing errors, suggests that they might be conspecific or closely related sister species.

Analyses of the individual partitions identified JC+1 for ITS rDNA, TIM2e+G4 for *TEF1*, TNe+G4 for *RPB1*, and TIM2e+G4 for *RPB2* as the optimal models of molecular evolution based on the Bayesian information criterion (BIC) scores (Chernomor et al. 2016) using ModelFinder (Kalyaanamoorthy et al. 2017). A partitioned ML-BS analysis of the combined data set, based on 5000 pseudoreplicates, provided strong support (ML-BS = 97–100%) for the six genealogically exclusive lineages represented by two or more strains (FIG. 1, TABLE 2). These six lineages were also strongly supported as monophyletic by a MP-BS analysis of the 4-gene data set (MP-BS = 100%; FIG. 1, TABLE 2). In the ML and MP analyses, a monotypic lineage represented by *Fusarium* sp. NRRL 66739 = FRC L-0453 from an unknown source in China was resolved as a putative sister to *F. sublunatum* from soil in Costa Rica in analyses of the four individual (SUPPLEMENTARY FIGS. 2–5) and the combined (FIG. 1) data set. To further evaluate its phylogenetic status, maximum parsimony analyses of alignments of 20 individual genes mined from the genomes of *F. sublunatum* NRRL 13384 and *Fusarium* sp. NRRL 66739, and the combined 60.4 kb data set, revealed that divergence between these putative sister lineages ranged from 0.9% to 5.2%, with an overall divergence of 1.75% across the concatenated 60.4 kb data set (TABLE 4).

ML-BS and MP-BS analyses of the combined 4-gene data set (FIG. 1) support the recognition of seven phylogenetically distinct species within the FBSC. Of the four newly discovered phylospecies, *F. abutilonis*, a putative pathogen of weedy members of the Malvaceae and Fabaceae in North America and soil in New Caledonia, and *F. guadeloupense* from soil in Guadeloupe and human blood in Texas are formally described below. The two unnamed phylospecies include *Fusarium* sp. NRRL 66179/66182 from *Hibiscus moscheutos* (rose or swamp mallow) from Washington State (Lupien et al. 2017) and the monotypic lineage represented by *Fusarium* sp. NRRL 66739 from China (TABLE 1). Except for one node along the backbone of the phylogeny, which was poorly resolved (FIG. 1; ML-BS/MP-BS = 57%/68%), all other evolutionary relationships were strongly supported (ML-BS/MP-BS = 97–100%/100%). *Fusarium abutilonis* + *Fusarium* sp. NRRL 66179/66182 from *H. moscheutos* and *F. sublunatum* + *Fusarium* sp. NRRL 66739 were resolved as sisters. In addition, two subclades were identified (FIG. 1): *F. buharicum* + (*F. abutilonis* + *Fusarium* sp. NRRL 66179/66182) and *F. convolutans* from soil rhizosphere in South Africa + (*F. sublunatum* + *Fusarium* sp. NRRL 66739). By contrast, phylogenetic relationships of *F. guadeloupense* NRRL 36125/66743 and the two subclades were unresolved. Of these, *F. buharicum, F. abutilonis*, and *Fusarium* sp. NRRL 66179/66182 are the only species within the FBSC that are known to be phytopathogenic, and they all have been reported to induce disease on malvaceous hosts (TABLE 1).

Determination of and secondary metabolite biosynthetic potential.— antiSMASH analysis revealed the presence of genes required for biosynthesis of some mycotoxins in the genome sequences of some members of the FBSC (SUPPLEMENTARY TABLE 1). The 16-gene fumonisin biosynthetic gene cluster was detected in *Fusarium* sp. NRRL 66182. The trichothecene biosynthetic gene (*TRI*) cluster was present in *Fusarium* sp. NRRL 66739, but the cluster consisted of only eight of the 10–14 genes that are described in *TRI* clusters in other

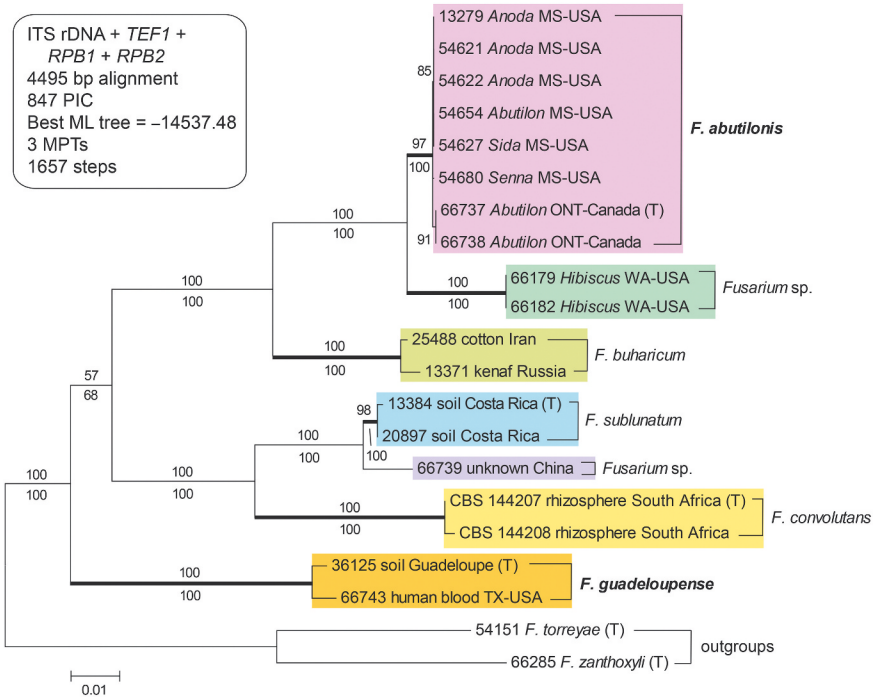

Figure 1. Partitioned maximum likelihood (ML) phylogeny of the *Fusarium buharicum* species complex (FBSC) inferred from aligned sequences from portions of four loci totaling 4495 bp conducted with IQ-TREE 1.6.12 (Nguyen et al. 2015). The phylogeny was rooted on sequences of two outgroup species in the *F. torreyae* species complex based on prior analyses (O'Donnell et al. 2013). Numbers above and below nodes represent ML and maximum parsimony bootstrap values (MP-BS), respectively, based on 5000 pseudoreplicates of the data. Thickened internodes identify six species lineages strongly supported by bootstrapping. The phylogenetic results support recognition of seven phylospecies within the FBSC, including *F. abutilonis* and *F. guadeloupense* (in bold font) formally described herein. Strains identified by a 5-digit number are accessioned in the ARS Culture Collection (NRRL). CBS = Westerdijk Fungal Biodiversity Institute culture collection; MPTs = most parsimonious trees; PIC = parsimony-informative character; T = ex-type strain.

fusaria (Alexander et al. 2009). Two genes of the beauvericin (enniatin) biosynthetic gene cluster were present in *Fusarium* sp. NRRL 66182 and *F. guadeloupense* NRRL 36125. There was also a partial fusaric acid biosynthetic cluster in NRRL 66182. Genes required for biosynthesis of the mycotoxins fusarins and zearalenone were not detected in any of the FBSC genome sequences examined. Genes required for biosynthesis of several other *Fusarium* metabolites that are not considered mycotoxins were also detected in some or all the FBSC genome sequences examined. These metabolites included the plant hormone auxin, carotenoid and fusarubin pigments, and the siderophores ferricrocin and fusarinine (SUPPLEMENTARY TABLE 1). Biosynthetic genes for the pigment bikaverin (Busman et al. 2012) were also detected in *Fusarium* sp. NRRL 66739 but not in other strains. A complete equisetin biosynthetic gene cluster was detected in *F. sublunatum* NRRL 13384, and a partial cluster was detected in *Fusarium* sp. NRRL 66739. Equisetin biosynthetic genes were not detected in other strains examined (SUPPLEMENTARY TABLE 1), but equisetin was detected in maize cultures of the two strains of *F. sublunatum* tested (9.88–13.02 ng/mL; TABLE 1).

TAXONOMY

Fusarium abutilonis Gräfenhan, Nirenberg & Seifert, sp. nov. FIG. 2

MycoBank MB838628

Typification: CANADA. ONTARIO: On *Abutilon theophrasti* (**holotype** BPI 924391, dried culture of NRRL 66737, Herbarium of US National Fungus Collection, USA, designated in this study). Collector and collection date unknown. Ex-type culture NRRL 66737 = DAOMC 213370.

Etymology: Based on one of the hosts, *Abutilon theophrasti*.

Diagnosis: Genealogical exclusive sister to *Fusarium* sp. NRRL 66179/66182 based on multilocus molecular phylogenetic analyses. A putative leaf, stem, and root rot pathogen of weedy members of Malvaceae and Fabaceae, also isolated from soil. Colonies 34–44 mm

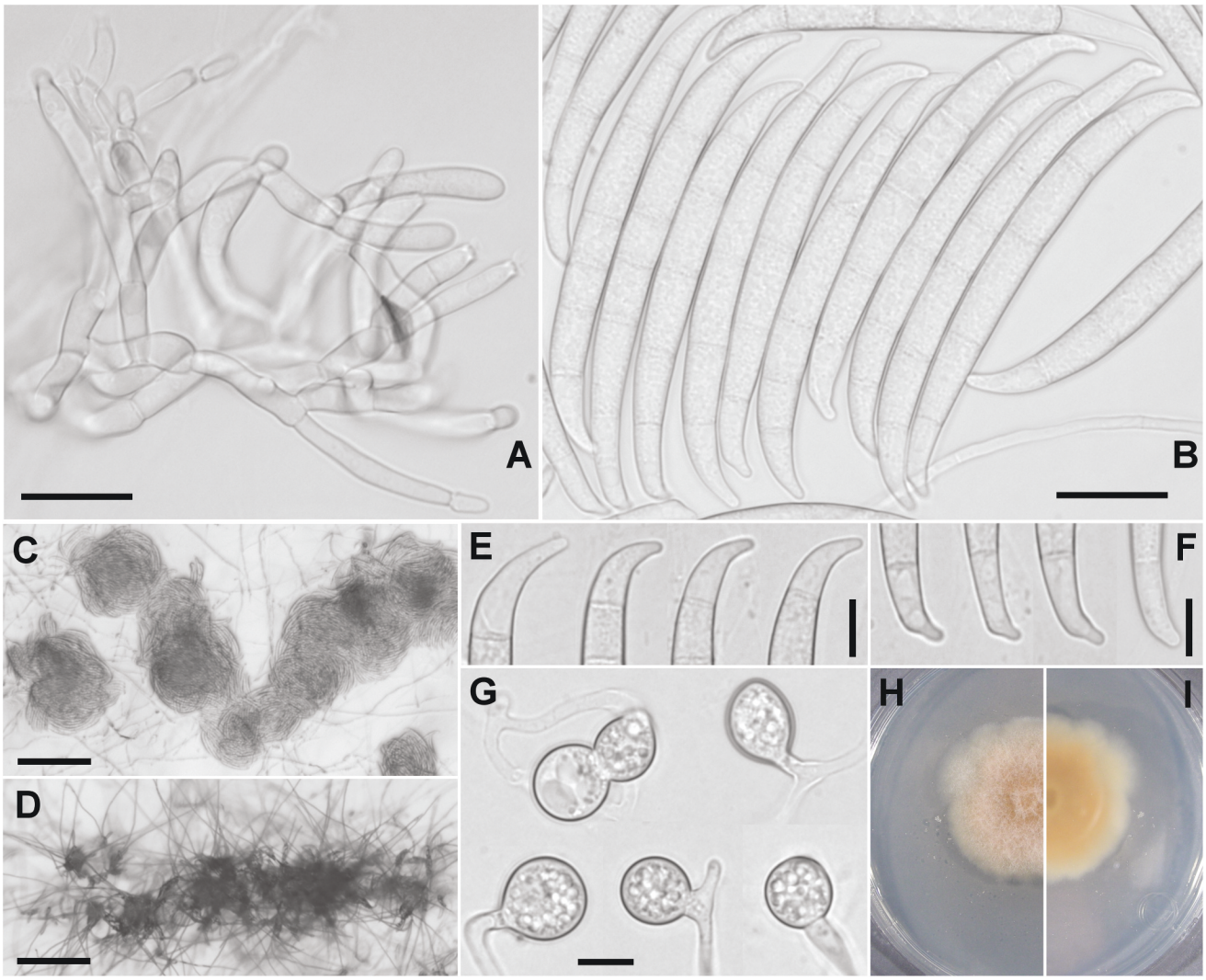

Figure 2. *Fusarium abutilonis* cultured under a 12 h dark/12 h near-UV black and white fluorescent light cycle at 25 C on SNA. A. Conidiophores with phialides. B. Sporodochial conidia. C–D. Sporodochial conidia on agar surface and in aerial mycelium. E, F. Apical and basal cells of sporodochial conidia. G. Chlamydospores. H, I. Colony surface and reverse. Bars: A–B = 20 µm; C–D = 200 µm; E–G = 10 µm.

radius after 7 d on PDA; sporodochia pale orange. Sporodochial conidia larger than in most *Fusarium* species, mostly 5-septate, 64–85 × 7–9 µm; microconidia and chlamydospores sparse or absent.

Observations on PDA: Fast-growing wild-type colony radius 34–44 mm after 7 d under black light at 25 C; degenerate colonies only grew 15–28 mm during the same time frame. Wild-type colony reverse orange (7A4), sometimes turning grayish brown (7E3) or grayish blue (21E6) in the center. Surface smooth or slightly mealy, orange (6A7), sometimes turning grayish brown (7E3) in the center, aerial mycelium white (1A1), sparse to slightly lanose to cottony, margin transparent or white. Sporodochia in older colonies up to 1 mm diam, occasionally coalescing into larger, irregular conidial masses up to 1 cm in diam, conidial masses dark to dull blue (21F3–23E3) turning yellow in 85% lactic acid.

Observations on SNA: On agar with filter paper putatively mutated slow-growing colony radius 13–22 mm after 7 d under near-UV black and white fluorescent light at 25 C. Colonies transparent, sporodochia produced on filter paper or on surrounding agar at first pale orange (5A3). Phialides 15.5–23.5 × 4–5 µm, cylindrical or slightly swollen, periclinal thickening visible, collarette slightly flared. Sporodochial conidia mostly 5-septate, 54–87 × 7.5–9 µm (n = 62), sometimes 4-septate (48–72 × 5.5–8.5 µm, n =7) or 6-septate (73.5–89 × 6–8 µm, n = 4), almost straight to curved, walls parallel in the center, apical cell conical and slightly hooked, about the same length as or slightly longer than the penultimate cell, basal cell with a relatively distinct foot. Conidia absent or sparsely produced in aerial mycelium on SNA and PDA in ambient light: 1-septate aerial conidia 15 × 3.5–4 µm, 2-septate aerial conidia 25.5–29

× 4–5 µm, and 3-septate aerial conidia 34 × 5 µm observed among larger sporodochial conidia. Aerial conidia 21–30 × 1.5–4 µm, produced from lateral solitary phialides on hyphae of aerial mycelium, or fascicles of hyphae. Chlamydospores sparse, single or in chains of up to 6, intercalary or terminal, hyaline, globose, 10–20 µm diam.

Distribution: Ontario, Canada; Mississippi, USA; Port Laguerre, New Caledonia.

Additional strains studied: See TABLE 1.

Notes: The blue color of the sporodochial conidia of *F. abutilonis* grown under some conditions is unusual in *Fusarium* but is also seen in members of the *Fusarium solani* species complex and in the potato pathogen *F. coeruleum*. In the FBSC, it was also reported in *F. buharicum* by Gerlach and Nirenberg (1982). We are not aware of other observations of these pigments turning yellow in lactic acid, but pH-sensitive red or blue pigments are well known in stromata and perithecia of the Hypocreales (Samuels 1973).

Fusarium guadeloupense Gräfenhan, Nirenberg & Seifert, sp. nov. FIG. 3

MycoBank MB838630

Typification: GUADELOUPE. Soil (**holotype** BPI 924391, dried culture of NRRL 36125, Herbarium of US National Fungus Collection, USA, designated in this study). Collector and collection date unknown. Ex-type culture NRRL 36125 = CBS 102302 = BBA 70872.

Etymology: Based on type locality in Guadeloupe.

Diagnosis: Genealogical exclusive lineage within *F. buharicum* species complex; however, its precise phylogenetic relationship with six other species within this complex unresolved by molecular phylogenetic analyses of a 4-gene data set. Colonies 41–43 mm radius after 7 d on PDA; sporodochia pale orange; sporodochial conidia larger than in most *Fusarium* species, mostly 5-septate, 41.5–63 × 5–6 µm. Microconidia absent. Chlamydospores present.

Observations on PDA: Colonies very fast-growing, radius 41–43 mm after 7 d under near-UV black and white fluorescent light at 25 C. Colony reverse orange (6B4–7B5) with grayish brown (7E4) spots 1–4 mm in diam, sporodochia immersed in medium. Surface white (1A1) to reddish gray (8A1–8B2), aerial mycelium white (1A1) to reddish gray (8A1–8B2), dense, cottony up to 6 mm high. Sporodochia up to 2 mm in diam, sometimes coalescing into larger, irregular conidial masses up to 5 mm in diam, conidial masses yellowish brown (5D5–5D6).

Observations on SNA: On agar with filter paper fast-growing, radius 37–45 mm after 7 d under near-UV black and white fluorescent light at 25 C. Colonies transparent, aerial mycelium on SNA with filter paper occasionally lanate, sporodochia at first light to grayish orange (6A2–6B2), produced on filter paper or directly on and in agar up to 2 mm in diam. Phialides 13–24 × 2–5 µm (n = 30), cylindrical or slightly swollen, periclinal thickening usually visible. Sporodochial conidia mostly 5-septate, 41.5–63 × 5–6 µm (n = 50), rarely 6-septate (68 × 6 µm, n = 1), almost straight to slightly curved, dorsal surface more curved than ventral surface, broadest at or slightly above the center, apical cell conical and slightly bent, about the same length as or slightly longer than the penultimate cell, foot of the basal cell not as distinct as in *F. abutilonis*. Chlamydospores single or in chains, intercalary or terminal, hyaline, mostly globose, 7.5–11.5 µm diam (n = 30).

Distribution: Guadeloupe and Texas, USA.

Additional strain examined: NRRL 66743 = UTHSC DI14-24 from human blood, Texas, USA.

Notes: The two strains of *Fusarium guadeloupense*, NRRL 36125 and NRRL 66743, did not produce microconidia in yeast-malt broth cultures, and 3-d-old cultures grown at 25 C only grew 1.9 mm/d when they were transferred to 37 C.

DISCUSSION

The present study represents the most detailed assessment of evolutionary relationships and species diversity within the FBSC to date. GCPSR-based analyses of three of the four individual partitions and the combined 4-gene data set strongly support recognizing seven species within the FBSC (TABLE 2, FIG. 1). Although analyses of the ITS rDNA, with only 27 PICs, did not resolve *F. abutilonis* and *F. buharicum* as genealogically exclusive (SUPPLEMENTARY FIG. 5), it did not contradict their monophyly. Therefore, these analyses fulfill operational criteria of genealogical concordance and nondiscordance under GCPSR (Dettman et al. 2003; Taylor et al. 2000). Because monophyly of the monotypic lineage represented by *Fusarium* sp. NRRL 66739 could not be assessed by bootstrapping, maximum parsimony analyses of the 4-gene data set (mean divergence = 1.3%; TABLE 3) and 20 full-length genes mined from whole genome sequence data (mean divergence = 1.75%; TABLE 4; Geiser et al. 2021) support recognition of this monotypic lineage as a phylogenetically divergent sister of *F. sublunatum*.

In prior morphological taxonomic treatments, members of what is now recognized as the FBSC, *F. buharicum* and *F. sublunatum*, were placed in section Discolor (Gerlach and Nirenberg 1982; Wollenweber and Reinking 1935) or treated as and insufficiently documented in this section (Nelson et al. 1983), or not illustrated (Leslie and Summerell 2006). Booth (1971)

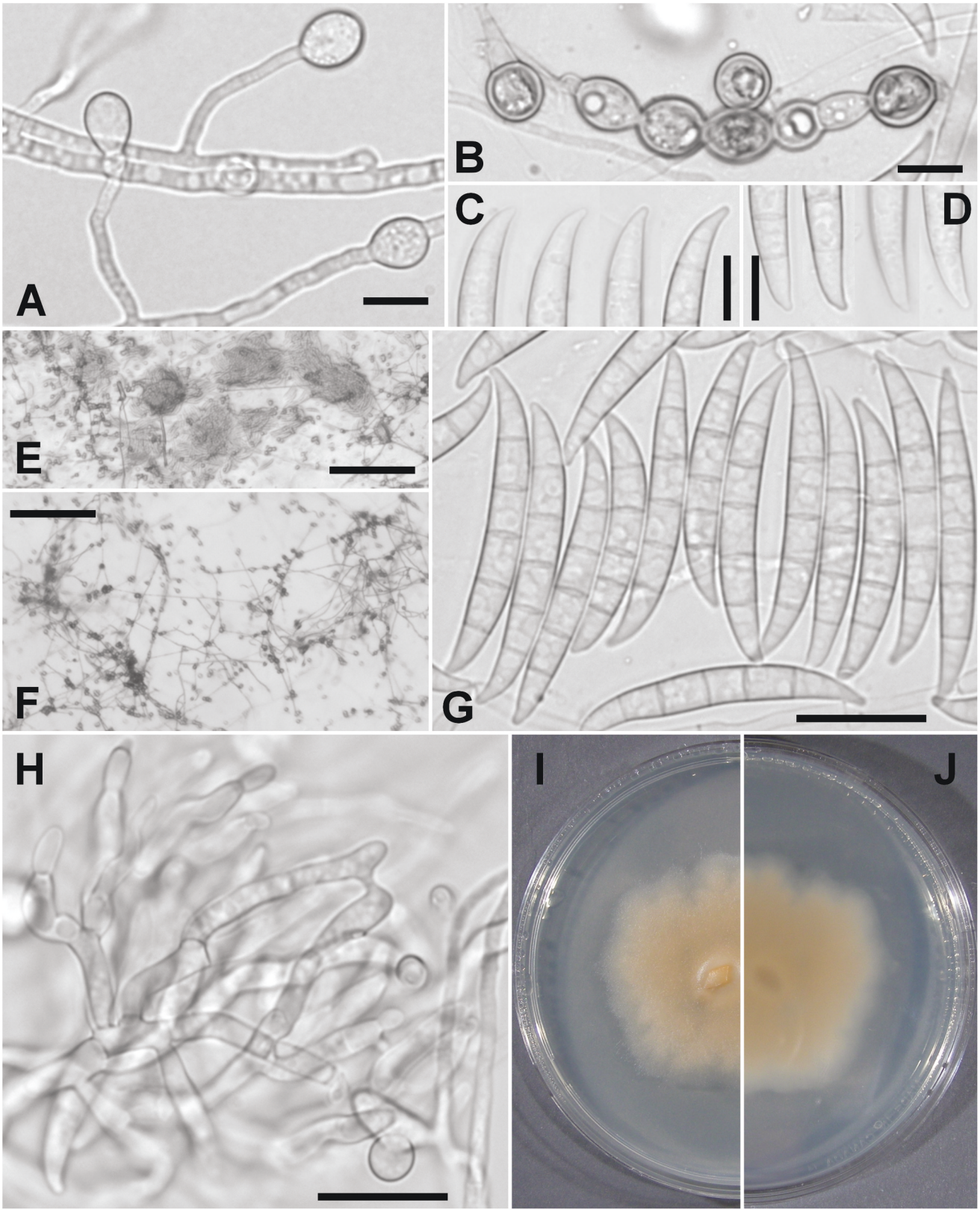

Figure 3. *Fusarium guadeloupense* cultured under a 12 h dark/12 h near-UV black and white fluorescent light cycle at 25 C on SNA. A, B. Chlamydospores in aerial mycelium and substrate. C, D. Apical and basal cells of sporodochial conidia. E. Sporodochia on agar surface. F. Aerial mycelium with chlamydospores. G. Sporodochial conidia. H. Conidiophores with phialides. I, J. Colony surface and reverse. bars: A–D = 10 µm; E–F = 200 µm.

placed *F. buharicum* in section Discolor but did not include *F. sublunatum*. Section Discolor was established by Wollenweber (1913) to include fusaria that produce thick-walled sporodochial conidia that are fusiform to falcate with a beaked to fusoid apical cell and an apedicellate or pedicellate foot cell, chlamydospore production, and the absence of microconidia. In morphological terms, the species of the FBSC are like those of the *F. sambucinum* species complex, which includes the majority of other species previously attributed to section Discolor.

The two species formally described herein, *F. abutilonis* and *F. guadeloupense*, share several morphological characters with other members of the FBSC, including slow to moderate growth rates, production of robust, thick-walled sporodochial conidia with pedicellate foot cells, chlamydospores, and a relative sparseness of microconidia. The number of septa in most sporodochial conidia and the range in their lengths and their widths are useful diagnostic morphological characters for distinguishing the five formally described Buharicum clade species when cultured on SNA with filter paper at 25 C. *Fusarium convolutans*, the only member of the FBSC reported from the African continent, is unique in that it is the only species in this complex that produces mostly 3-septate conidia; it also produces abundant sterile, coiled hyphae in vitro. With 3-septate conidia measuring 25.5–38.5 µm, these are shorter than the predominately 5-septate sporodochial conidia of the four other species. The length ranges of the 5-septate conidia of *F. abutilonis* (64–85 µm) and *F. guadeloupense* (41.5–63 µm) can be used to distinguish these two sister species. The conidia of *F. abutilonis* are 7.5–9 µm wide, and among the broadest in the genus. However, the length ranges of *F. guadaloupense* overlaps with the sporodochial conidia produced by *F. buharicum* (typically 45–65 µm) and *F. sublunatum* (48–66 µm) (Gerlach and Nirenberg 1982; Wollenweber and Reinking 1935). The macroconidia of *F. guadaloupense* and *F. buharicum* have similar shapes, but the macroconidia of *F. sublunatum* are more falcate than those of the other Buharicum clade species and sometimes have a more extended foot on the basal cell.

The subtle morphological differences of these species are reflected by the fact that three of the FBSC were not recognized as novel when originally deposited in culture collections: *F. abutilonis* as *F. tumidum* and *Fusarium* sp. NRRL 66739 as *F. lateritium* in the Fusarium Research Center, Pennsylvania State University (Walker 1981), and *F. guadeloupense* as *F. sublunatum* in the Institute for Epidemiology and Pathogen Diagnostics Culture Collection, Berlin, Germany (BBA 70872 = CBS 102302). The FRC misidentifications are attributed in part because Nelson et al. (1983) employed an overly broad morphological concept of *F. lateritium, F. tumidum*, and other fusaria that only produce unusually large sporodochial conidia. This also explains Nelson's misidentification of *F. torreyae* as *F. lateritium* (Aoki et al. 2013).

The FBSC phylogeny inferred from the combined data set resolved a clade comprising three species that induce disease symptoms on malvaceous hosts, including cotton and kenaf (*F. buharicum*), rose or swamp mallow (*Fusarium* sp. NRRL 66179/66172; Lupien et al. 2017), and three invasive weeds in North America (*F. abutilonis*). The latter species was reported as *F. lateritium* pathogenic to several other members of the Malvaceae and the leguminous weed sicklepod (*Senna obtusifolia*), inducing leaf, stem, and root lesions (Walker 1981). It remains to be determined whether the four other *F. buharicum* clade species are phytopathogenic. None were isolated from symptomatic plants, and three were recovered from soil, including *F. sublunatum* in Costa Rica and Panama (Wollenweber and Reinking 1935), *F. guadeloupense* in New Caledonia, and *F. convolutans* in South Africa (Sandoval-Denis et al. 2018).

The second strain of *F. guadeloupense* NRRL 66743 was recovered from human blood in Texas and deposited in the Fungus Testing Laboratory, University of Texas Health Science Center at San Antonio, as *Fusarium* sp. UTHSC DI14-24. This finding is noteworthy because it represents the only human isolate of *Fusarium* known to us that produces abundant chlamydospores but no microconidia in yeast-malt broth cultures and the only representative of the FBSC implicated in a human infection (Zhang et al. 2015). Given the novelty of this putative mycotic agent, which exhibited slow growth at 37 C, future studies are needed to assess the extent to which it can infect humans and other animals.

Fumonisins and trichothecenes are among the mycotoxins of most concern to food and feed safety. Although fumonisin and trichothecene biosynthetic gene clusters were detected in the genome sequences of *Fusarium* spp. NRRL 66182 and NRRL 66739, respectively, production of economically important analogs of these mycotoxins families was not detected in cracked maize kernel cultures of either strain. It is not clear why the mycotoxins were not detected, but it is possible that the maize kernel medium was not conducive to production in these taxa. In addition, the absence of the *TRI1, TRI7*, and *TRI13* genes in the trichothecene gene cluster of *Fusarium* sp. NRRL 66739 could account for the absence of

production of nivalenol, deoxynivalenol, and T-2 toxin, which require one or more of these genes for their biosynthesis. We are currently conducting a more extensive analysis of NRRL 66739 to determine whether it produces novel trichothecene analogs. The presence of fumonisin, trichothecene, fusaric acid, equisetin, and bikaverin biosynthetic gene clusters in the genome sequences of members of the FBSC was not expected because surveys of these genes indicate that they are present in distantly related species complexes (Brown and Proctor 2016; Kim et al. 2020; O'Donnell et al. 2013). Indeed, the presence of the clusters is not surprising given evidence for multiple occurrences of horizontal transfer of biosynthetic gene clusters among *Fusarium* species complexes (Kim et al. 2020; Proctor et al. 2013; Villani et al. 2019). The discovery that the two strains of *F. sublunatum* NRRL 13384 and 20897 produced the tetramic acid analog equisetin (Sims et al. 2005) represents the first report of toxin production within this species complex. Marasas et al. (1984), Munkvold (2017), and Munkvold et al. (2021) did not include members of the FBSC in their reviews of toxigenic *Fusarium* species. Equisetin is a cytotoxic antibiotic that acts on protein membranes and hydrophobic domains in a nonspecific manner (König et al. 1993) and is produced by phylogenetically diverse species within *Fusarium* (Kim et al. 2020). Confirming the report of Schütt et al. (1998), we also did not detect moniliformin production in solid cracked maize cultures of *F. buharicum* and *F. sublunatum*, and the other FBSC tested.

In summary, two genealogically exclusive members of the FBSC discovered in the present study, *F. abutilonis* and *F. guadeloupense*, were formally described here. Although future studies are needed to determine whether two undescribed species, *Fusarium* sp. ex *Hibiscus moscheutos* from Washington, USA (Lupien et al. 2017), and *Fusarium* sp. NRRL 66739 from China, can be distinguished using morphological data, we recommend using partial sequences from a phylogenetically informative gene (*TEF1, RPB1*, or *RPB2*) to obtain a definitive species identification by conducting BLASTn queries of FUSARIUM-ID 3.0 (Torres-Cruz et al. 2022) and NCBI GenBank (O'Donnell et al. 2022). This recommendation is based in part on results of BLASTn searches of GenBank, using ITS rDNA sequences as the queries, that indicate the FBSC likely comprises more species than included in the present study. No sexual cycle has been reported for any member of the FBSC, but this could be due to scientists encountering this group on a rare basis, as evidenced by the relatively few known FBSC isolates available in culture. Karyotype evolution within the FBSC appears to be another fertile area of research: despite genomes of *F. buharicum* NRRL 13371 and *F. sublunatum* NRRL 13384 genomes having similar estimated sizes (36.1 vs. 35.7 Mb, respectively), germ tube burst method (GTMB)-based karyotyping revealed that they possess 9 + 1 and 18–20 chromosomes, respectively (Waalwijk et al. 2018). Given that 5/7 species within the Buharicum clade were discovered within the past 5 years (Lupien et al. 2017; Sandoval-Denis et al. 2018; present study), GCPSR-based analyses of multilocus DNA sequence data from phylogenetically diverse fusaria have and will continue to greatly advance our knowledge of evolutionary relationships among and species diversity within this agronomically important group of mycotoxigenic plant pathogens (Summerell 2019).

ACKNOWLEDGMENTS

The authors would like to thank Amy McGovern, Crystal Probyn, Ethan Roberts, and Deborah S. Shane for skilled assistance in various aspects of this study. T.G. and K.A. S. are grateful for contributions by Helgard I. Nirenberg in the early stages of this project. Thanks are due to the Canadian Collection of Fungal Cultures (DAOM, Ottawa) and the Institute for Epidemiology and Pathogen Diagnostics Culture Collection (Julius Kühn-Institute, Berlin) for providing cultures.

Disclaimer: Mention of trade names or commercial products in this publication is solely for the purpose of providing specific information and does not imply recommendation or endorsement by the US Department of Agriculture (USDA). USDA is an equal opportunity provider and employer.

DISCLOSURE STATEMENT

No potential conflict of interest was reported by the author(s).

FUNDING

This research was supported in part by the US Department of Agriculture, Agricultural Research Service National Program for Food Safety, National Science Foundation (NSF) grant DEB-1655980, Pennsylvania State Agricultural Experiment Station Project 4655, and CRTI project 04-0045RD. I.L. was supported in part by an appointment to the ARS Research Participation Program administered by the Oak Ridge Institute for Science and Education (ORISE) through an interagency agreement between the US Department of Energy (DOE) and the US Department of Agriculture (USDA). ORISE is managed by ORAU under DOE contract number DE-SC0014664. All opinions expressed in this paper are the authors' and do not necessarily reflect the policies and views of USDA, DOE, or ORAU/ORISE.

ORCID

Kerry O'Donnell http://orcid.org/0000-0001-6507-691X
Tom Gräfenhan http://orcid.org/0000-0002-3653-4851

Imane Laraba http://orcid.org/0000-0002-2118-8773
Mark Busman http://orcid.org/0000-0001-9750-064X
Robert H. Proctor http://orcid.org/0000-0001-5400-1680
Hye-Seon Kim http://orcid.org/0000-0002-9747-1591
Nathan P. Wiederhold http://orcid.org/0000-0002-2225-5122
David M. Geiser http://orcid.org/0000-0002-1590-2045
Keith A. Seifert http://orcid.org/0000-0001-8877-4796

LITERATURE CITED

Alexander NJ, Proctor RH, McCormick SP. 2009. Genes, gene clusters, and biosynthesis of trichothecenes and fumonisins in *Fusarium*. Toxin Rev. 28:198–215.

Aoki T, O'Donnell K, Geiser DM. 2014. Systematics of key phytopathogenic *Fusarium* species: current status and future challenges. J Gen Plant Pathol. 80:189–201.

Aoki T, Smith JA, Mount LL, Geiser DM, O'Donnell K. 2013. *Fusarium torreyae* sp. nov., a pathogen causing canker disease of Florida torreya (*Torreya taxifolia*), a critically endangered conifer restricted to northern Florida and southwestern Georgia. Mycologia. 105:312–19.

Aoki T, Vaughan MM, McCormick SP, Busman M, Ward TJ, Kelly A, O'Donnell K, Johnston PR, Geiser DM. 2015. *Fusarium dactylidis* sp. nov., a novel nivalenol toxin-producing species sister to *F. pseudograminearum* isolated from orchard grass (*Dactylis glomerata*) in Oregon and New Zealand. Mycologia. 107:409–18.

Blin K, Wolf T, Chevrette MG, Lu X, Schwalen CJ, Kautsar SA, Suarez Duran HG, de Los Santos ELC, Kim HU, Nave M, et al. 2017. antiSMASH 4.0-improvements in chemistry prediction and gene cluster boundary identification. Nucleic Acids Res. 45:W36–W41.

Booth C. 1971. The genus *Fusarium*. Kew (UK): Commonwealth Mycological Institute. 237 p.

Brown DW, Proctor RH. 2016. Insights into natural products biosynthesis from analysis of 490 polyketide synthases from *Fusarium*. Fungal Genet Biol. 89:37–51.

Busman M. 2017. Utilization of high performance liquid chromatography coupled to tandem mass spectrometry for characterization of 8-*O*-methylbostrycoidin production by species of the fungus *Fusarium*. J Fungi. 3:43.

Busman M, Butchko RA, Proctor RH. 2012. LC-MS/MS method for the determination of the fungal pigment bikaverin in maize kernels as an indicator of ear rot. Food Addit Contam Part A. 29:1736–42.

Chernomor O, von Haeseler A, Minh BQ. 2016. Terrace aware data structure for phylogenomic inference from supermatrices. Syst Biol. 65:997–1008.

Dettman JR, Jacobson DJ, Taylor JW. 2003. A multilocus genealogical approach to phylogenetic species recognition in the model eukaryote *Neurospora*. Evolution. 57:2703–20.

Edgar RC. 2004. MUSCLE: multiple sequence alignment with high accuracy and high throughput. Nucleic Acids Res. 32:1792–97.

Gardes M, Bruns TD. 1993. ITS primers with enhanced specificity for basidiomycetes— application to the identification of mycorrhizae and rusts. Mol Ecol. 2:113–18.

Geiser DM, Al-Hatmi A, Aoki T, Arie T, Balmas V, Barnes I, Bergstrom GC, Bhattacharyya MKK, Blomquist CL, Bowden R, et al. 2021. Phylogenomic analysis of a 55.1 kb 19-gene dataset resolves a monophyletic *Fusarium* that includes the *Fusarium solani* Species Complex. Phytopathology. 111:1064–79.

Geiser DM, Aoki T, Bacon CW, Baker SE, Bhattacharyya MK, Brandt ME, Brown DW, Burgess LW, Chulze S, Coleman JJ, et al. 2013. Letter to the Editor: one fungus, one name: defining the genus *Fusarium* in a scientifically robust way that preserves longstanding use. Phytopathology. 103:400–08.

Geiser DM, Del Mar Jimenez-gasco M, Kang S, Makalowska I, Veeraraghavan N, Ward TJ, Zhang N, Kuldau GA, O'Donnell K. 2004. FUSARIUM-ID v. 1.0: a DNA sequence database for identifying *Fusarium*. Eur J Plant Pathol. 110:473–79.

Gerlach W, Nirenberg HI. 1982. The genus *Fusarium*—a pictorial atlas. Mitteilungen aus der Biologischen Bundesanstalt für Land- und Forstwirtschaft. Berlin-Dahlem. 209:1–406.

Gerlach W, Scharif G. 1970. Der Erreger einer Fußkrankheit an *Hibiscus cannabinus* in Iran—*Fusarium buharicum* Jaczewski. Phytopathologische Z. 68:323–33.

Gouy M, Guindon S, Gascuel O. 2009. SeaView version 4: a multiplatform graphical user interface for sequence alignment and phylogenetic tree building. Mol Biol Evol. 27:221–24.

Gräfenhan T, Johnston PR, Vaughan MM, McCormick MM, Proctor RH, Busman M, Ward TJ, O'Donnell K. 2016. *Fusarium praegraminearum* sp. nov., a novel nivalenol mycotoxin-producing pathogen from New Zealand can induce head blight on wheat. Mycologia. 108:1229–39.

Jaczewski AA. 1929. Some diseases of cotton fibres. Rev Appl Mycol. 9:159–67.

Kalyaanamoorthy S, Minh BQ, Wong TKF, von Haeseler A, Jermiin LS. 2017. ModelFinder:fast model selection for accurate phylogenetic estimates. Nat Methods. 14:587–89.

Kim H-S, Lohmar JM, Busman M, Brown DW, Nauman TA, Divon HH, Lysoe E, Uhlig S, Proctor RH. 2020. Identification and distribution of gene cluster required for synthesis of sphingolipid metabolism inhibitors in *Fusarium*. BMC Genom. 21:50.

König T, Kapus A, Sarkadi B. 1993. Effects of equisetin on rat liver mitochondria: evidence for inhibition of substrate anion carriers of the inner membrane. J Bioenerg Biomembr. 25:537–45.

Kornerup A, Wanscher JH. 1978. Methuen handbook of color. 3rd ed. London (UK): Methuen; p. 252.

Laraba I, Busman M, Geiser DM, O'Donnell K. 2022. Phylogenetic diversity and mycotoxin potential of emergent phytopathogens within the *Fusarium tricinctum* species complex. Phytopathology. doi:10.1094/PHYTO-09-21-0394-R

Laraba I, Keddad A, Boureghda H, Abdallah N, Vaughan MM, Proctor RH, Busman M, O'Donnell K. 2018. *Fusarium algeriense*, sp. nov., a novel toxigenic crown rot pathogen of durum wheat from Algeria is nested in the *Fusarium burgessii* species complex. Mycologia. 109:935–50.

Laraba I, McCormick SP, Vaughan MM, Geiser DM, O'Donnell K. 2021. Phylogenetic diversity, trichothecene potential, and pathogenicity within *Fusarium sambucinum*

species complex. PLoS One. doi:10.1371/journal.pone.0245037
Leslie JF, Summerell BA. 2006. The *Fusarium* laboratory manual. Ames (Iowa): Blackwell Professional Publishing. 388 p.
Liu YJ, Whelen S, Hall BD. 1999. Phylogenetic relationships among ascomycetes: evidence from an RNA polymerase II subunit. Mol Biol Evol. 16:1799–808.
Lupien SL, Dugan FM, Ward KM, O'Donnell K. 2017. Wilt, crown, and root rot of common rose mallow (*Hibiscus moscheutos*) caused by a novel *Fusarium* sp. Plant Dis. 101:354–58.
Marasas WFO, Nelson PE, Toussoun TA. 1984. Toxigenic *Fusarium* species: identity and mycotoxicology. University Park (PA): Pennsylvania State University Press. 328 p.
Munkvold GP. 2017. *Fusarium* species and their associated mycotoxins. In: Moretti A, Susca A, editors. Mycotoxigenic fungi: methods and protocols. New York (NY): Humana Press; p. 51–106.
Munkvold GP, Proctor RH, Moretti A. 2021. Mycotoxin production in *Fusarium* according to contemporary species concepts. Annu Rev Phytopathol. 59:373–402.
Nelson PE, Toussoun TA, Marasas WFO. 1983. *Fusarium* species: an illustrated manual for identification. University Park: Pennsylvania State University Press. 193 p.
Nguyen L-T, Schmidt HA, von Haeseler A, Minh BQ. 2015. IQ-TREE: a fast and effective stochastic algorithm for estimating maximum-likelihood phylogenies. Mol Biol Evol. 32:268–74.
Niehaus EM, Munsterkotter M, Proctor RH, Brown DW, Sharon A, Idan Y, Oren-Young L, Sieber CM, Novak O, Pencik A, et al. 2016. Comparative "Omics" of the *Fusarium fujikuroi* species complex highlights differences in genetic potential and metabolite synthesis. Genome Biol Evol. 8:3574–99.
Nirenberg H, O'Donnell K. 1998. New *Fusarium* species and combinations within the *Gibberella fujikuroi* species complex. Mycologia. 90:434–58.
Nirenberg HI. 1976. Untersuchungen über die morphologische und biologische Differenzierung in der *Fusarium*-Sektion *Liseola*. Mitteilungen aus der Biologischen Bundesanstalt für Land- und Forstwirtschaft. Berlin-Dahlem. 169:1–117.
O'Donnell K. 2000. Molecular phylogeny of the *Nectria haematococca-Fusarium solani* species complex. Mycologia. 92:919–38.
O'Donnell K, Cigelnik E, Nirenberg HI. 1998a. Molecular systematics and phylogeography of the *Gibberella fujikuroi* species complex. Mycologia. 90:465–93.
O'Donnell K, Gueidan C, Sink S, Johnston PR, Crous PW, Glenn A, Riley R, Zitomer NC, Colyer P, Waalwijk C, et al. 2009. A two-locus DNA sequence database for typing plant and human pathogens within the *Fusarium oxysporum* species complex. Fungal Genet Biol. 46:936–48.
O'Donnell K, Kistler HC, Cigelnik E, Ploetz RC. 1998b. Multiple evolutionary origins of the fungus causing Panama disease of banana: concordant evidence from nuclear and mitochondrial gene genealogies. Proc Natl Acad Sci USA. 95:2044–49.
O'Donnell K, Rooney AP, Proctor RH, Brown DW, McCormick SP, Ward TJ, Frandsen RJ, Lysøe E, Rehner SA, Aoki T, et al. 2013. Phylogenetic analyses of *RPB1* and *RPB2* support a middle Cretaceous origin for a clade comprising all agriculturally and medically important fusaria. Fungal Genet Biol. 52:20–31.
O'Donnell K, Sutton DA, Rinaldi MG, Sarver BA, Balajee SA, Schroers HJ, Summerbell RC, Robert VA, Crous PW, Zhang N, et al. 2010. Internet-accessible DNA sequence database for identifying fusaria from human and animal infections. J Clin Microbiol. 48:3708–18.
O'Donnell K, Ward TJ, Robert VARG, Crous PW, Geiser DM, Kang S. 2015. DNA sequence-based identification of *Fusarium*: current status and future directions. Phytoparasitica. 43:583–95.
O'Donnell K, Whitaker B, Laraba I, Proctor RH, Brown D, Broders K, Kim H-S, McCormick SP, Busman M, Aoki T, et al. 2022. DNA sequence-based identification of *Fusarium*: a work in progress. Plant Dis. doi:10.1094/PDIS-09-21-2035-SR
Proctor RH, Van Hove F, Susca A, Stea G, Busman M, van der Lee T, Waalwijk C, Moretti A, Ward TJ. 2013. Birth, death and horizontal transfer of the fumonisin biosynthetic gene cluster during the evolutionary diversification of *Fusarium*. Mol Microbiol. 90:290–306.
Reeb V, Lutzoni F, Roux C. 2004. Contribution of *RPB2* to multilocus phylogenetic studies of the euascomycetes (Pezizomycotina, Fungi) with special emphasis on the lichen-forming *Acarosporaceae* and evolution of polyspory. Mol Phylogenet Evol. 32:1036–60.
Reinking OA. 1934. Interesting new fusaria. Zentralbl Bakteriol Parasitenkd Infektionskr Hyg. 89:509–14.
Samuels GJ. 1973. The genus *Macbridella* with notes on *Calostilbe, Herpotrichia, Phaeonectria*, and *Letendraea*. Can J Bot. 51:1275–83.
Sandoval-Denis M, Crous PW. 2018. Removing chaos from confusion: assigning names to common human and animal pathogens in *Neocosmospora*. Persoonia. 41:109–29.
Sandoval-Denis M, Swart WJ, Crous PW. 2018. New *Fusarium* species from the Kruger National Park, South Africa. MycoKeys. 34:63–92.
Schütt F, Nirenberg HI, Deml G. 1998. Moniliformin production in the genus *Fusarium*. Mycotoxin Res. 14:35–40.
Sims JW, Fillmore JP, Warner DD, Schmidt EW. 2005. Equisetin biosynthesis in *Fusarium heterosporum*. Chem Comm. 14(2):186–88. Epub 2004 Nov 22. PMID: 15724180. doi:10.1039/b413523g.
Stanke M, Morgenstern B. 2005. AUGUSTUS: a web server for gene prediction in eukaryotes that allows user-defined constraints. Nucleic Acids Res. 33:W465–W467.
Summerell BA. 2019. Resolving *Fusarium*: current status of the genus. Annu Rev Phytopathol. 57:323–39.
Taylor JW, Jacobson DJ, Kroken S, Kasuga T, Geiser DM, Hibbett DS, Fisher MC. 2000. Phylogenetic species recognition and species concepts in fungi. Fungal Genet Biol. 31:21–32.
Torres-Cruz TJ, Whitaker BK, Proctor RH, Broders K, Laraba I, Kim H-S, Brown DW, O'Donnell K, Estrada-Rodríguez TL, Lee Y-H, et al. 2022. FUSARIUM-ID v.3.0: an updated, downloadable resource for *Fusarium* species identification. Phytopathology. doi:10.1094/PDIS-09-21-2105-SR
Villani A, Proctor RH, Kim HS, Brown DW, Logrieco AF, Amatulli MT, Moretti A, Susca A. 2019. Variation in secondary metabolite production potential in the *Fusarium*

incarnatum-equiseti species complex revealed by comparative analysis of 13 genomes. BMC Genom. 20:314.

Waalwijk C, Taga M, Zheng S-L, Proctor RH, Vaughan MM, O'Donnell K. 2018. Karyotype evolution in *Fusarium*. IMA Fungus. 9:13–26.

Walker HL. 1981. *Fusarium lateritium*: a pathogen of spurred anoda (*Anoda cristata*), prickly sida (*Sida spinosa*), and velvetleaf (*Abutilon theophrasti*). Weed Sci. 29:629–31.

White TJ, Bruns T, Lee S, Taylor JW. 1990. Amplification and direct sequencing of fungal ribosomal genes for phylogenetics. In: Innis MA, Gelfand DH, Sninsky JJ, White TJ, editors. PCR protocols: a guide to methods and applications. San Diego (California): Academic Press; p. 315–22.

Wollenweber HW. 1913. Studies on the *Fusarium* problem. Phytopathology. 3:24–50.

Wollenweber HW, Reinking OA. 1935. Die Fusarien, ihre Beschreibung, Schadwirkung und Bekämpfung. Berlin (Germany): Paul Parey. 355 p.

Yilmaz N, Sandoval-Denis M, Lombard L, Visagie CM, Wingfield BD, Crous PW. 2021. Redefining species limits in the *Fusarium fujikuroi* species complex. Persoonia. 46:129–62.

Zhang SX, O'Donnell K, Sutton DA. 2015. *Fusarium* and other opportunistic hyaline fungi. In: Jorgensen JH, Pfaller MA, Carroll KC, Funke G, Landry ML, Richter SS, Warnock DW, editors. Manual of clinical microbiology. Washington (DC): ASM Press; p. 2057–86.

Zhou X, O'Donnell K, Kim H-S, Proctor RH, Doehring G, Cao Z-M. 2018. Heterothallic sexual reproduction in three canker-inducing tree pathogens within the *Fusarium torreyae* species complex. Mycologia. 110:710–25.